Journal of Pure and Applied Sciences (JPAS),
Volume 2, Issue 2, Page 135-148, 2026

Density–Porosity–Property Relationships in Zirconia-, Spinel-, and Silicon Carbide-Modified AZS Refractory Ceramics

S. Shado[1*], C. A. Kenneth-Emehige[2]

[1,2]Department of Glass and Ceramic Technology, The Federal Polytechnic Ado-Ekiti, Ekiti State, Nigeria.
[1]shado_as@fedpolyado.edu.ng, [2]amaracomfort@gmail.com
*Corresponding author (Email: shado_as@fedpolyado.edu.ng , Phone: +2348060422079)

ABSTRACT

Alumina–zirconia–silica (AZS) refractories are widely used in high-temperature industrial applications because of their excellent thermal stability, corrosion resistance, and mechanical strength. This study investigated the effects of zirconia, spinel, and silicon carbide additions on the physical and mechanical properties of AZS refractory ceramics. Four compositions comprising Standard AZS (Batch A), Zr-rich AZS (Batch B), Spinel AZS (Batch C), and SiC AZS (Batch D) were developed and evaluated in terms of bulk density, relative density, apparent porosity, water absorption, elastic modulus, compressive strength, hardness, and flexural strength. The results showed that zirconia enrichment significantly improved densification and mechanical performance. Batch B exhibited the highest bulk density (3.78 g/cm³), relative density (0.900), elastic modulus (197.1 GPa), compressive strength (189.9 MPa), hardness (10.18 GPa), and flexural strength (96.4 MPa), while also recording the lowest apparent porosity (5.5%) and water absorption (1.45%). Conversely, Batch D showed the lowest density and mechanical properties and the highest porosity and water absorption. Correlation analysis revealed strong inverse relationships between porosity and density, stiffness, strength, hardness, and flexural strength, confirming that densification and porosity control are critical determinants of refractory performance. The overall performance ranking was Batch B > Batch A > Batch C > Batch D, indicating that zirconia enrichment is an effective approach for enhancing the structural integrity, durability, and service performance of AZS refractory ceramics in demanding high-temperature environments.

***Keywords*— Alumina–Zirconia–Silica (AZS) Refractories; Zirconia Enrichment; Densification and Porosity; Mechanical Properties; High-Temperature Ceramics**

I. INTRODUCTION

Alumina–zirconia–silica (AZS) refractories are among the most widely used ceramic materials in glass furnaces and other high-temperature industrial environments because of their excellent corrosion resistance, thermal stability, and mechanical strength. The performance of these refractories is strongly influenced by their densification behaviour, which governs porosity, microstructural integrity, and resistance to mechanical and thermal degradation. Densification is largely controlled by compositional design, as the

type and concentration of additives affect sintering kinetics, phase evolution, grain bonding, and pore elimination during firing. Previous studies have demonstrated that zirconia plays a significant role in enhancing densification and mechanical performance in zircon-based ceramic systems. Zirconia additions improve sintering behaviour through enhanced mass transport and phase interactions, resulting in increased density and reduced porosity [1]. Compositional modifications can promote liquid-phase-assisted densification and improve the mechanical properties of zircon-containing ceramics [2]. Zirconia-rich ceramic systems exhibit improved thermal stability and structural integrity due to stronger interfacial bonding and reduced susceptibility to microcrack formation [3]. These studies highlight the importance of zirconia in improving the densification and service performance of refractory materials. In addition to zirconia, other additives such as spinel-forming oxides and silicon carbide have been employed to modify refractory behaviour.

Optimized oxide compositions can improve microstructural development and densification through enhanced diffusion pathways during sintering [4], [5]. However, excessive secondary-phase formation may also introduce residual porosity and influence the final mechanical properties. The relationship between composition and mechanical performance has been widely reported, with increased densification generally leading to improvements in elastic modulus, hardness, strength, and thermal shock [6–8]. Since porosity acts as a stress concentrator and crack initiation site, reducing pore content remains a critical requirement for achieving superior refractory performance. Despite extensive studies on zircon-based ceramics, comparative information on the effects of zirconia enrichment, spinel formation, and silicon carbide incorporation within AZS refractory systems remains limited. Understanding how these compositional modifications influence densification, porosity, and mechanical performance is essential for developing refractory materials capable of operating under severe service conditions.

Therefore, this study investigates the effect of zirconia-, spinel-, and silicon carbide-based modifications on the densification behaviour and mechanical properties of AZS refractory ceramics. The objective of this study is to identify the composition that provides the optimum combination of high density, low porosity, superior strength, stiffness, hardness, and flexural performance for high-temperature refractory applications.

II. MATERIALS AND METHODS

A. Material Preparation

The oxide raw materials employed in this investigation were procured from a reputable chemical supplier in Akure, Ondo State, Nigeria. The materials included high-purity alumina (Al_2O_3), silica (SiO_2), magnesium oxide (MgO), and silicon carbide (SiC). While zircon (ZrSiO4) was purchased in Jos, Plateau state. Prior to processing, each powder was dried in a laboratory oven at 110°C for 12 h to eliminate adsorbed moisture and prevent agglomeration during mixing. Moisture removal is essential because retained water can adversely affect powder flowability, particle packing, and the reproducibility of ceramic processing operations [9]. Following drying, the powders were weighed according to the formulations shown in Table 1 and table 2 using an analytical balance with an accuracy of ±0.001 g. The weighed powders were then transferred into zirconia milling jars and subjected to wet ball milling in ethanol for 6 h using zirconia grinding media. Wet milling was selected because it improves particle dispersion, reduces agglomeration, and promotes homogeneous mixing of constituent phases. Ethanol was employed as the milling medium because of its low surface tension, rapid evaporation characteristics, and ability to minimize contamination during processing [10]. The milled slurry was subsequently dried at 80°C to evaporate the ethanol and recover the mixed powder. The dried powder was then gently crushed and sieved through a 75 μm mesh sieve to obtain a uniform particle size distribution suitable for pressing. Uniform particle size distribution improves packing efficiency and promotes uniform densification during sintering [11].

B. Batch Calculations for Test Specimens

To prepare specimens of approximately 50 mm × 50 mm × 50 mm, the total batch weight for each composition was adjusted to produce sufficient material for compaction and machining. Based on the measured dry specimen masses obtained experimentally, the average dry masses were: Consolidated Batch Composition and Material Requirements for a Single Specimen.

Table 1. Batch Formulations of Experimental AZS Refractories (wt.%)

Batch ID	Al_2O_3	ZrSiO4	SiO_2	MgO (Spinel Precursor)	SiC (Particulate)
A – Standard AZS (Baseline)	60	30	10	0	0
B – Zr-rich AZS	50	40	10	0	0
C – Spinel-Reinforced AZS	55	30	10	5	0
D – SiC-Enhanced AZS	55	30	10	0	5

Table 2. Batch compositions and raw material proportions of the developed AZS refractory formulations used in the study.

Batch ID	Description	Dry Weight (g)	Al_2O_3 (g)	ZrSiO4 (g)	SiO_2 (g)	MgO (g)	SiC (g)	Total (g)
A	Standard AZS (Baseline)	52.20	31.32	15.66	5.22	0.00	0.00	52.20
B	Zr-rich AZS	52.70	26.35	21.08	5.27	0.00	0.00	52.70
C	Spinel-Reinforced AZS	52.60	28.93	15.78	5.26	2.63	0.00	52.60
D	SiC-Enhanced AZS	52.40	28.82	15.72	5.24	0.00	2.62	52.40

Note: The material weights were calculated directly from the batch compositions and the experimentally adopted dry specimen weights (52.2–52.7 g) for the preparation of individual test specimens used in this study.

C. Specimen Forming

A 5 wt.% polyvinyl alcohol (PVA) solution was used as a temporary binder to improve green strength and facilitate handling after pressing. Approximately 4–6 wt.% binder solution was gradually added to each powder batch while mixing manually until a semi-plastic consistency was achieved. The prepared mixtures were uniaxially compacted in hardened steel moulds under a pressure of approximately 100–150 MPa to produce cubic specimens measuring 50 mm × 50 mm × 50 mm. Additional specimens were fabricated as ASTM C133 or ISO 5013 bars for flexural strength testing. The compacted specimens were carefully ejected from the moulds and air-dried for 24 h before further drying in an oven at 110°C for 12 hours.

D. Specimen Forming

A 5 wt.% polyvinyl alcohol (PVA) solution was used as a temporary binder to improve green strength and facilitate handling after pressing. Approximately 4–6 wt.% binder solution was gradually added to each powder batch while mixing manually until a semi-plastic consistency was achieved. The prepared mixtures were uniaxially compacted in hardened steel moulds under a pressure of approximately 100–150 MPa to produce cubic specimens measuring 50 mm × 50 mm × 50 mm. Additional specimens were fabricated as ASTM C133 or ISO 5013 bars for flexural strength testing. The compacted specimens were carefully ejected from the moulds and air-dried for 24 h before further drying in an oven at 110°C for 12 hours.

E. Sintering Procedure

The dried specimens were fired in an electrically heated high-temperature furnace. The firing schedule consisted of a controlled heating rate of 5°C min^{-1} up to 1300°C, followed by a soaking period of 2 h to

ensure adequate densification and phase development. After sintering, the furnace was allowed to cool naturally to room temperature. The selected firing temperature was chosen to promote bonding among alumina, zirconia, and silica phases while facilitating spinel formation in MgO-containing compositions and ensuring good matrix integration in SiC-containing samples. Previous studies have shown that densification and microstructural evolution in AZS refractories are strongly dependent on firing temperature and composition [12-13]. The fired specimens were subsequently characterized for bulk density, apparent porosity, water absorption, elastic modulus, hardness, strength, flexural strength, and firing shrinkage.

F. Characterization of samples

The fired refractory specimens were characterized for bulk density, apparent porosity, water absorption, hardness, flexural strength, and firing shrinkage. Physical properties were determined using the Archimedes immersion technique in accordance with standard ceramic testing procedures. Figure 1 shows the samples of the fired refractory crucible.

(i) Determination of Bulk Volume

The bulk volume of each specimen was determined using the Archimedes principle and calculated as:

$$\text{Bulk volume, } V = W_{sat} - W_{sus} \quad (1)$$

where: V = bulk volume (cm^3)

W_{sat} = saturated (wet) weight of specimen (g)

W_{sus} = suspended weight of specimen in water (g)

(ii) Determination of Bulk Density

Bulk density was calculated from the ratio of dry weight to bulk volume:

$$\text{Bulk density, } \rho_b = \frac{W_d}{W_{sat} - W_{sus}} \quad (2)$$

Where ρ_b = bulk density (g/cm^3)

W_d = dry weight of specimen (g)

W_{sat} = saturated weight (g)

W_{sus} = suspended weight in water (g)

Substituting Equation (2) into Equation (1):

Bulk volume, $V = \frac{W_d}{\rho_b}$ (3)

(iii) Determination of Apparent Porosity

The apparent porosity of the fired specimens was determined using:

$$P_a = \frac{W_{sat} - W_d}{W_{sat} - W_{sus}} \times 100 \quad (4)$$

Where P_a = apparent porosity (%)

W_{sat} = saturated weight (g)

W_d = dry weight (g)

W_{sus} = suspended weight (g)

(iv) Determination of Water Absorption

Water absorption was calculated as:

Water Absorption, $WA = \frac{W_{sat} - W_d}{W_d} \times 100$ (5)

Where WA = water absorption (%)

W_{sat} = saturated weight (g)

W_d = dry weight (g)

Figure 1: Photographs of the Fired refractory Crucible Samples

III. RESULTS AND DISCUSSION

Figure 2 shows that zirconia, spinel, and silicon carbide additions significantly influenced the physical and mechanical properties of the developed AZS refractories. Overall performance followed the order: Batch B (Zr-rich AZS) > Batch A (Standard AZS) > Batch C (Spinel AZS) > Batch D (SiC AZS). Batch B exhibited the highest bulk density (3.78 g/cm³) and relative density (0.900), indicating superior densification and stronger grain bonding, while Batch D showed the lowest values (3.47 g/cm³ and 0.826), reflecting higher residual porosity. Apparent porosity ranged from 5.5% to 13.3%, and water absorption from 1.45% to 3.82%, with Batch B recording the lowest values and Batch D the highest.

These results indicate that zirconia enrichment enhanced sintering and reduced pore connectivity, whereas SiC addition promoted higher pore formation. Mechanical properties closely followed the densification trend. Elastic modulus ranged from 168.6 to 197.1 GPa, with Batch B exhibiting the highest stiffness due to its lower porosity and improved microstructural compactness. Similarly, compressive strength, hardness, and flexural strength increased with density and decreased with porosity. Batch B achieved the highest compressive strength (189.9 MPa), hardness (10.18 GPa), and flexural strength (96.4 MPa), while Batch D recorded the lowest values. The enhanced performance of Batch B is attributed to improved densification, reduced pore content, and zirconia-induced toughening. Overall, the results demonstrate that densification and porosity control are the primary factors governing AZS refractory performance. The superior combination of density, strength, stiffness, hardness, and low porosity obtained in Batch B highlights the effectiveness of zirconia enrichment in improving refractory durability and structural integrity. Consequently, the Zr-rich AZS composition is considered the most suitable formulation for high-temperature refractory applications.

A. Relationship Between Densification Parameters and Mechanical Properties of Developed AZS Refractories

Figure 3 shows a strong inverse relationship between bulk density and apparent porosity. As bulk density increased from 3.47 g/cm³ (Batch D) to 3.78 g/cm³ (Batch B), porosity decreased from 13.3% to 5.5%, indicating improved densification and pore elimination. Batch B exhibited the most compact microstructure, whereas Batch D contained the highest pore concentration. This trend agrees with reports that enhanced sintering improves particle packing, grain bonding, and densification, resulting in lower porosity and superior refractory performance [9], 10], [13], [14].

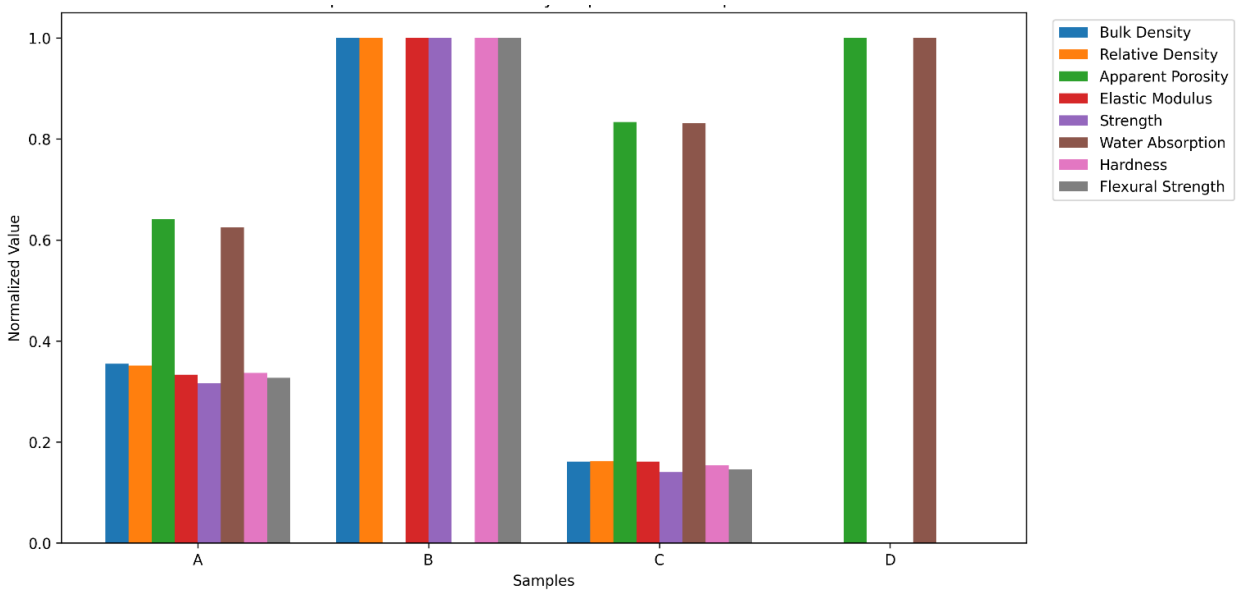

Figure 2: Comparison of normalized physical and mechanical properties of the developed AZS refractory compositions (Samples A–D)

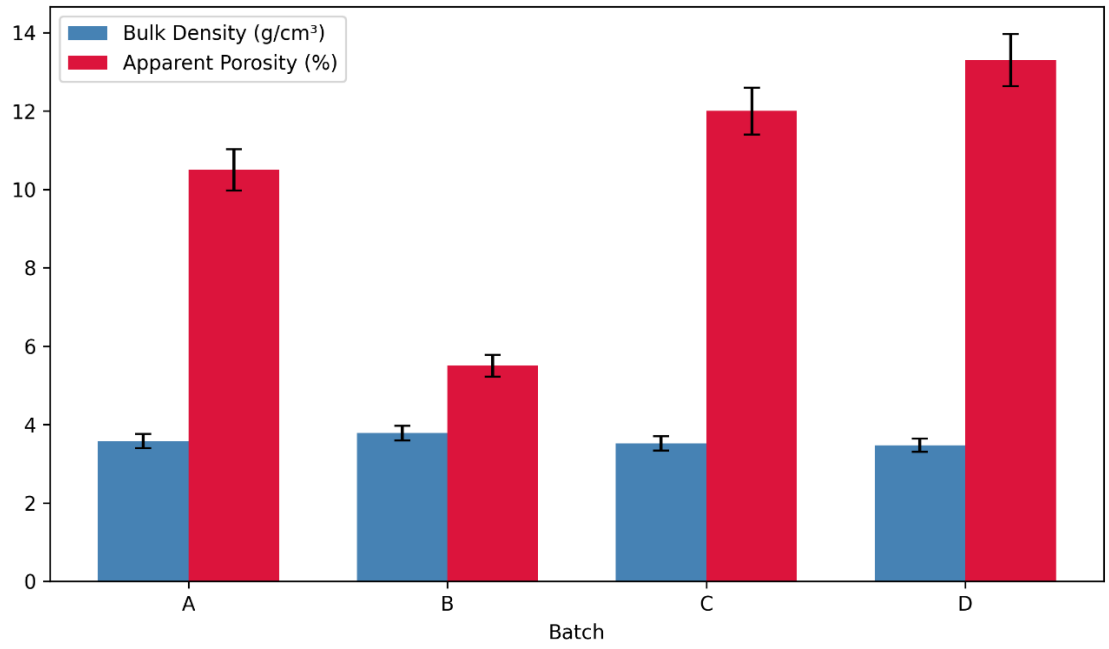

Figure 3: Relationship Between Bulk Density and Apparent Porosity of the Developed AZS Refractories

Figure 4 shows a strong inverse relationship between bulk density and water absorption. Batch B exhibited the highest density (3.78 g/cm³) and lowest water absorption (1.45%), while Batch D showed the lowest density (3.47 g/cm³) and highest absorption (3.82%). This indicates that denser refractories contain fewer interconnected pores available for water penetration. Previous studies have shown that water absorption decreases with increasing density and reduced pore connectivity, improving resistance to slag penetration and chemical attack [9], [13], [14], [15]. Figure 5 demonstrates that relative density increases as apparent porosity decreases. Batch B recorded the highest relative density (0.900) and lowest porosity (5.5%), whereas Batch D exhibited the lowest relative density (0.826) and highest porosity (13.3%). The results confirm that improved densification reduces residual pore volume and enhances consolidation. Similar relationships have been reported in ceramic systems, where porosity reduction is the primary mechanism for achieving high relative density and improved properties [9], [10], [14], [16].

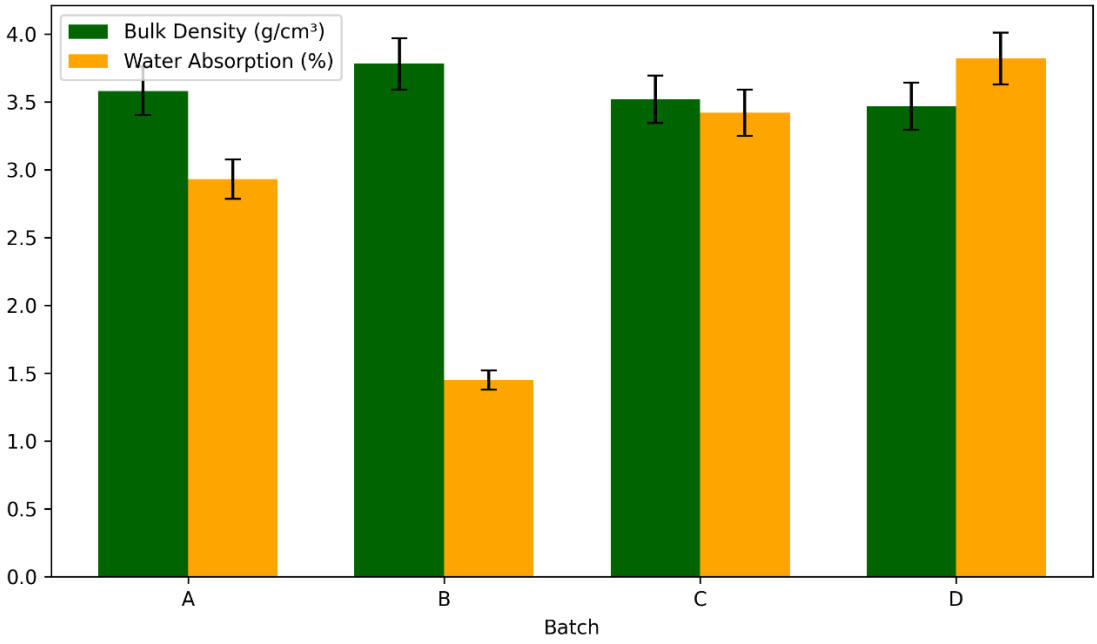

Figure 4: Relationship Between Bulk Density and Water Absorption of the Developed AZS Refractories

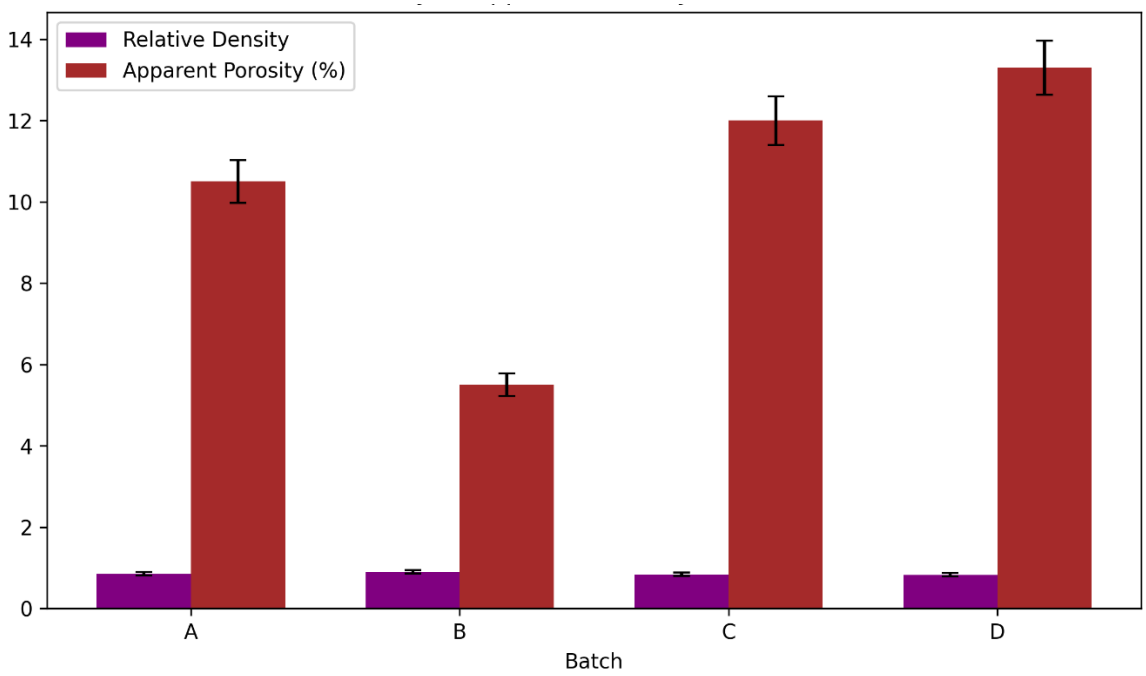

Figure 5: Correlation Between Relative Density and Apparent Porosity of the Developed AZS Refractories

Figure 6 shows that elastic modulus increased as porosity decreased. Batch B exhibited the highest modulus (197.1 GPa) at the lowest porosity (5.5%), while Batch D recorded the lowest modulus (168.6 GPa) at the highest porosity (13.3%). This indicates that pores reduce stiffness by interrupting stress transfer within the ceramic matrix. The trend supports the porosity–modulus relationship proposed by [17] and agrees with studies showing that improved densification enhances ceramic stiffness and elastic behaviour [9], [14], [18]. Figure 7 reveals a pronounced inverse relationship between compressive strength and porosity. As porosity decreased from 13.3% to 5.5%, strength increased from 128.6 MPa to 189.9 MPa. Reduced porosity improves load-bearing capacity by minimizing crack initiation sites. This observation agrees with studies showing that pores act as stress concentrators and significantly reduce ceramic strength, while enhanced densification improves mechanical performance [10], [14], [19], [20].

Figure 8 shows that hardness increased from 8.04 GPa (Batch D) to 10.18 GPa (Batch B) as porosity decreased. Lower porosity enhances resistance to indentation by increasing the effective load-bearing area. Similar trends have been reported for dense zirconia-containing ceramics, where reduced pore concentration improves hardness and wear resistance [9], [14], [21], [22].

This study focused on selected physical and mechanical properties and did not evaluate important high-temperature characteristics such as thermal shock resistance, creep behaviour, refractoriness under load,

and slag corrosion resistance. In addition, only four compositions were examined under laboratory conditions, and advanced microstructural analyses (SEM, EDS, and XRD) were not performed. Future studies should include detailed microstructural characterization, thermal and corrosion testing, and industrial-scale validation to further optimize AZS refractory performance.

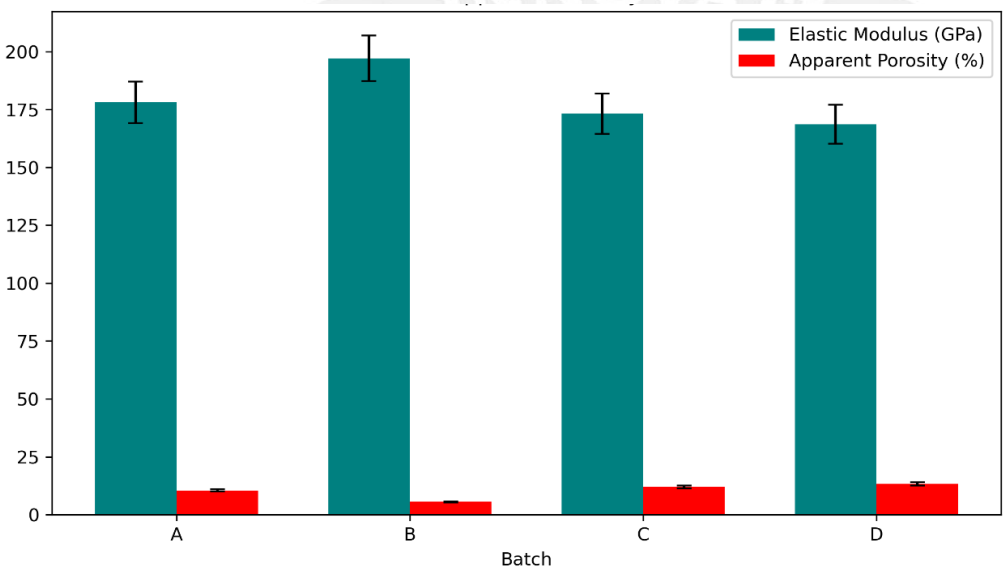

Figure 6: Relationship Between Elastic Modulus and Apparent Porosity of the Developed AZS Refractories

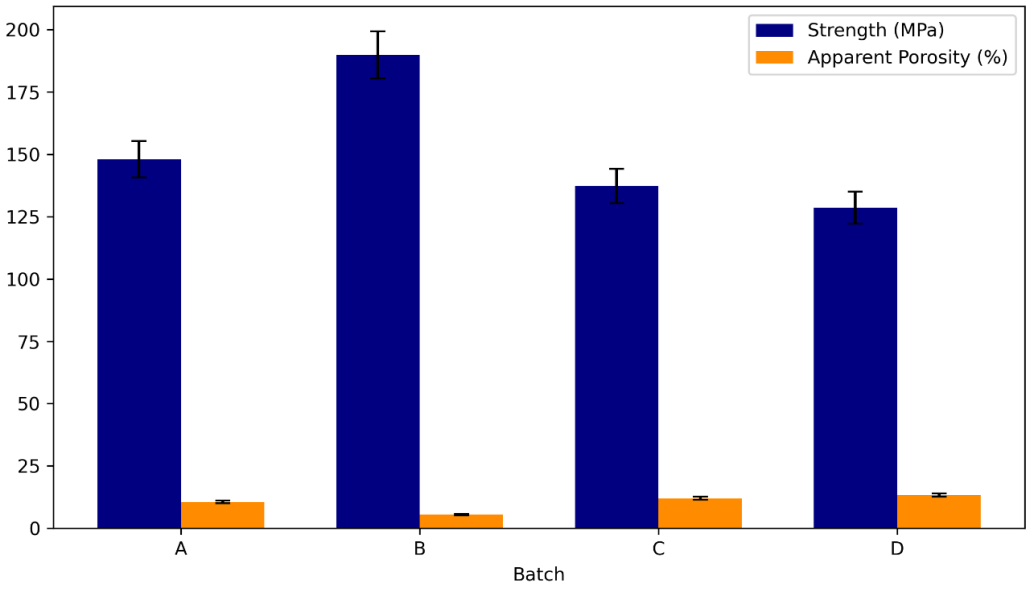

Figure 7: Relationship Between Compressive Strength and Apparent Porosity of the Developed AZS Refractories

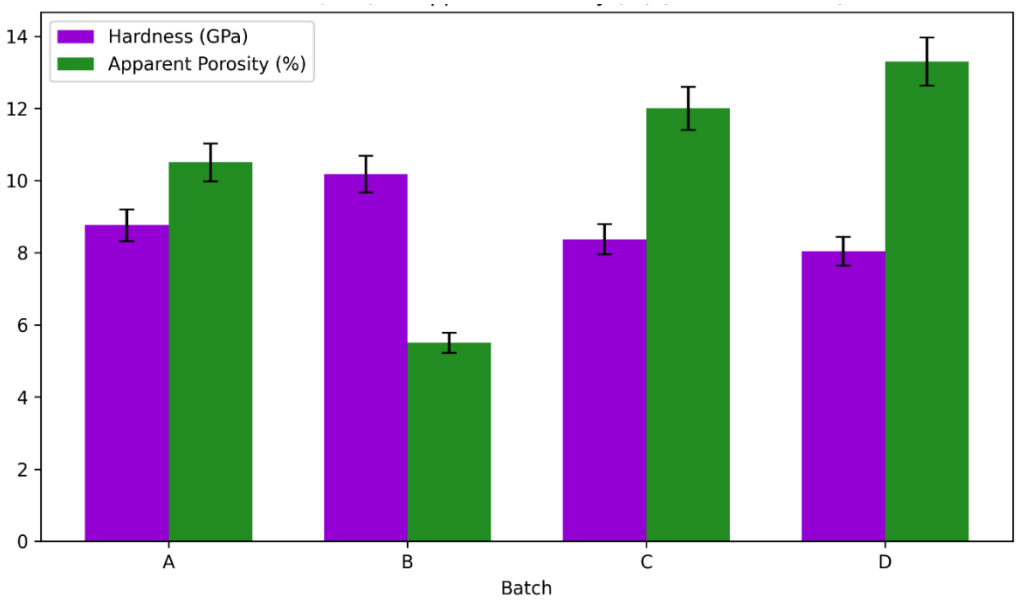

Figure 8: Relationship Between Hardness and Apparent Porosity of the Developed AZS Refractories

Figure 9 demonstrates that flexural strength increased with decreasing porosity. Batch B achieved the highest flexural strength (96.4 MPa) at 5.5% porosity, whereas Batch D recorded the lowest value (70.4 MPa) at 13.3% porosity. The results indicate that pores act as crack initiation sites during bending, thereby reducing fracture resistance. This finding is consistent with previous studies that identified porosity as a major factor controlling flexural strength and crack resistance in ceramics [10, [19], [22], [23].

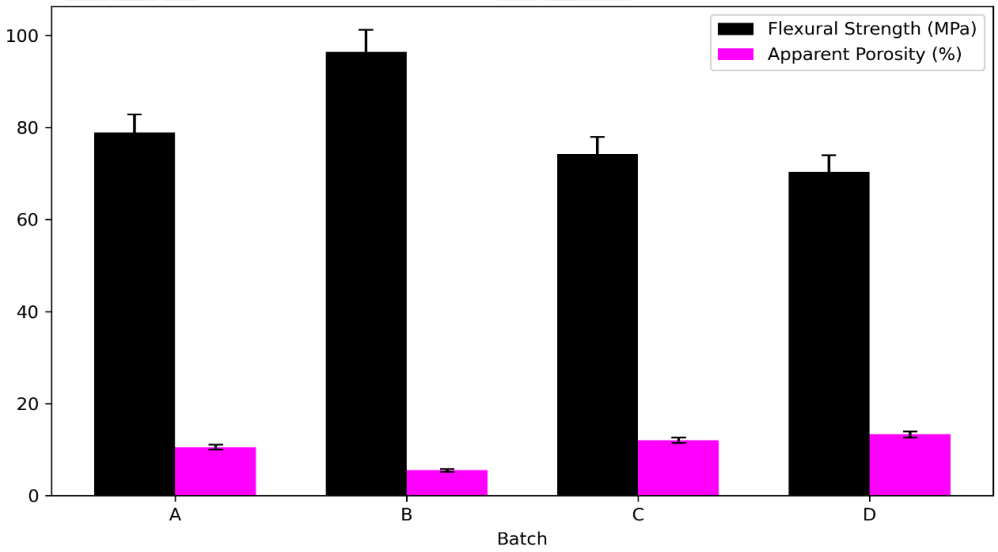

Figure 8: Relationship Between Flexural Strength and Apparent Porosity of the Developed AZS Refractories

IV. CONCLUSION

This study evaluated the effects of zirconia enrichment, spinel reinforcement, and silicon carbide addition on the densification and mechanical properties of AZS refractory ceramics. Among the compositions investigated, the Zr-rich AZS (Batch B) exhibited the best overall performance, characterized by the highest density, elastic modulus, compressive strength, hardness, and flexural strength, as well as the lowest porosity and water absorption. The improved properties were attributed to enhanced densification and reduced pore formation. Strong inverse relationships were observed between porosity and key engineering properties, confirming the importance of porosity control in refractory performance. Overall, the performance ranking was Batch B > Batch A > Batch C > Batch D, indicating that zirconia enrichment is the most effective modification for improving the structural integrity and durability of AZS refractories for high-temperature applications.

Acknowledgements

We would like to express our deepest gratitude to the Tertiary Education Trust Fund (TETFund) and Center for Research, Innovation and Development (CRID, Fed. Poly Ado-Ekiti) for their generous sponsorship and support of our study.

REFERENCES

[1] N. M. Rendtorff, S. Grasso, C. Hu, G. Suarez, E. F. Aglietti, and Y. Sakka, "Zircon–zirconia ($ZrSiO_4$–ZrO_2) dense ceramic composites by spark plasma sintering," J. Eur. Ceram. Soc., vol. 32, no. 4, pp. 787–793, 2012.

[2] V. Kumar, S. K. Nath, A. Ghosh, and H. S. Tripathi, "Effect of CaO addition on the sintering behaviour and mechanical properties of mullite–zirconia composites," Ceram. Int., vol. 42, no. 3, pp. 4351–4358, 2016.

[3] V. L. Ugolkov, V. I. Koval'chuk, and V. A. Osipov, "Phase stability and thermal resistance of zircon–zirconia ceramics with modified oxide interfaces," Ceram. Int., vol. 50, no. 1, pp. 121–132, 2024.

[4] M. M. S. Wahsh, R. M. Khattab, and M. Awaad, "Thermo-mechanical properties of mullite/zirconia reinforced alumina ceramic composites," Mater. Des., vol. 41, pp. 31–36, 2012.

[5] I. M. Bakr and M. M. Wahsh, "Influence of composition on the sintering behavior of alumina–magnesia–zircon composites," Ceram. Int., vol. 38, no. 7, pp. 5539–5546, 2012.

[6] N. M. Rendtorff, L. B. Garrido, and E. F. Aglietti, "Effect of zircon–zirconia ratio on mechanical and thermal properties," J. Mater. Sci., vol. 44, no. 22, pp. 6060–6068, 2009.

[7] T. Hemanth Raju, B. B. Chandan, B. Vinaya, S. Udayashankar, T. Jagadeesha, and A. K. Gajakosh, "Influence of zircon particles on the characterization of Al7050–zircon composites," Mater. Today: Proc., vol. 47, no. 10, pp. 2241–2246, 2021.

[8] J. Senthil, M. Kumar, C. Thiagarajan, and M. Prabhahar, "Synthesis and evaluation of zircon and Al_2O_3 zircon-reinforced AA6061 alloy composites in age-hardened condition," 2023.

[9] M. N. Rahaman, Ceramic Processing and Sintering, 2nd ed. New York, NY, USA: Marcel Dekker, 2003.

[10] W. D. Kingery, H. K. Bowen, and D. R. Uhlmann, Introduction to Ceramics, 2nd ed. New York, NY, USA: Wiley, 1976.

[11] J. S. Reed, Principles of Ceramics Processing, 2nd ed. New York, NY, USA: Wiley, 1995.

[12] W. E. Lee and R. E. Moore, "Evolution of in situ refractories in the twentieth century," J. Am. Ceram. Soc., vol. 81, no. 6, pp. 1385–1410, 1998.

[13] C. A. Schacht, Refractories Handbook. Boca Raton, FL, USA: CRC Press, 2004.

[14] R. W. Rice, Porosity of Ceramics: Properties and Applications. New York, NY, USA: Marcel Dekker, 1998.

[15] W. D. Callister Jr. and D. G. Rethwisch, Materials Science and Engineering: An Introduction, 10th ed. Hoboken, NJ, USA: Wiley, 2020.

[16] R. M. German, Powder Metallurgy and Particulate Materials Processing. Princeton, NJ, USA: Metal Powder Industries Federation, 2014.

[17] R. M. Spriggs, "Expression for effect of porosity on elastic modulus of polycrystalline refractory materials," J. Am. Ceram. Soc., vol. 44, no. 12, pp. 628–629, 1961.

[18] J. Kováčik, "Correlation between Young's modulus and porosity in porous materials," J. Mater. Sci. Lett., vol. 18, no. 13, pp. 1007–1010, 1999.

[19] E. Ryshkewitch, "Compression strength of porous sintered alumina and zirconia," J. Am. Ceram. Soc., vol. 36, no. 2, pp. 65–68, 1953.

[20] W. E. Lee and S. Zhang, "Melt corrosion of oxide and oxide–carbon refractories," Int. Mater. Rev., vol. 44, no. 3, pp. 77–104, 1999.

[21] C. Piconi and G. Maccauro, "Zirconia as a ceramic biomaterial," Biomaterials, vol. 20, no. 1, pp. 1–25, 1999.

[22] J. Chevalier, "What future for zirconia as a biomaterial?" Biomaterials, vol. 27, no. 4, pp. 535–543, 2006.

[23] A. S. Wagh, J. P. Singh, and R. B. Poeppel, "Dependence of ceramic fracture properties on porosity," J. Mater. Sci., vol. 28, no. 13, pp. 3589–3593, 1993.